Spectroelectrochemical studies and molecular orbital calculations on mononuclear complexes [Mo(Tp^{Me,Me})(NO)Cl(py)] (where py is a substituted pyridine derivative): electrochromism in the near-infrared region of the electronic spectrum

Ralph Kowallick, Andrew N. Jones, Zöe R. Reeves, John C. Jeffery, Jon A. McCleverty* and Michael D. Ward*

School of Chemistry, University of Bristol, Cantock's Close, Bristol, UK BS8 1TS. E-mail: mike.ward@bristol.ac.uk, jon.mccleverty@bristol.ac.uk

Received (in Cambridge, UK) 9th June 1999, Accepted 2nd July 1999

Reaction of [Mo(Tp^{Me,Me})(NO)Cl$_2$] [where Tp^{Me,Me} is hydrotris(3,5-dimethylpyrazolyl)borate] with substituted pyridine derivatives (py-R) affords the complexes [Mo(Tp^{Me,Me})(NO)Cl(py-R)] [**1**, R = 4-(1-butylpentyl); **2**, R = 4-Ph; **3**, R = 3-Ph; **4**, R = 4-benzoyl; **5**, R = 3-benzoyl; **6**, R = 4-acetyl; **7**, R = 3-acetyl; **8**, R = 4-cyano; **9**, R = 3-cyano; **10**, R = 4-Cl; **11**, R = 3-Cl; **12**, py-R = isoquinoline]. Two of the complexes, **5** and **8**, have been crystallographically characterised. These neutral, 17-electron complexes [formally Mo(I)] were examined by UV/VIS/NIR spectroelectrochemistry. All of them undergo a chemically reversible one-electron reduction to the 18-electron monoanion at potentials which are sensitive to the nature of the pyridyl substituent R. Whereas the neutral (17-electron) forms of the complexes only show transitions in the UV and visible regions of the spectrum of the type we have described before, the reduced forms of the complexes show intense, low-energy transitions ascribable to MLCT transition from the electron-rich metal centre [formally Mo(0)] to the π^* orbitals of the pyridyl ligands. The 4-substituted pyridines show only one such low-energy transition (*e.g.* for [**1**]$^-$, λ_{max} = 830 nm; ε = 12 000 dm^3 mol^{-1} cm^{-1}), but those complexes in which the pyridyl ligand has a strongly electron-withdrawing substituent at the C^3 position of the pyridyl ligand develop two new MLCT transitions on reduction of which one is well into the near-IR region: *e.g.* for complex [**5**]$^-$, λ_{max} = 717 nm; ε = 5300 dm^3 mol^{-1} cm^{-1} and λ_{max} = 1514 nm; ε = 2500 dm^3 mol^{-1} cm^{-1}. These spectroscopic results have been rationalised by ZINDO calculations which were used both to calculate the frontier molecular orbitals of the complexes, and to calculate the electronic spectra of the reduced complexes. The strong near-IR transitions in the reduced complexes with 3-substituted pyridines, especially [**5**]$^-$ and [**7**]$^-$, are of particular significance for the development of electrochromic dyes for use in electro-optic switching in this region of the spectrum.

We have recently been interested in the synthesis and study of redox-active metal complexes which in one oxidation state, have a strong absorbance in the near-infrared (NIR) region of the electromagnetic spectrum.[1] Such compounds are relatively rare examples of electrochromic NIR dyes,[2] which are of potential technological relevance in the areas of optical data storage and transmission, both of which rely on readily available semiconductor diode lasers which operate in the NIR region of the spectrum.[3]

In this paper we present the results of some spectroelectrochemical studies of simple mononuclear complexes of the form [Mo(Tp^{Me,Me})(NO)Cl(py)] [where Tp^{Me,Me} is hydrotris(3,5-dimethylpyrazolyl)borate, and py denotes a pyridine derivative or a related pyridine-like ligand]. These complexes are formally Mo(I) species with 17 valence electrons, and generally undergo two reversible metal-centred redox couples to afford the 16-electron cation by oxidation and the 18-electron anion by reduction.[4] Dinuclear complexes containing these fragments attached to either end of bis-pyridyl bridging ligands have been extensively studied by us, because of the strong electrochemical and magnetic exchange interactions that occur between the metal termini across the bridging ligand.[4–6] It now transpires that their electronic spectral properties are of interest because their reduced 18-electron forms show a strong absorbance which is at the red end of the visible region, or in some cases well into the NIR spectral region. We show in particular how the presence of an electron-withdrawing substituent in particular positions on the pyridyl ligand has a profound affect on the position and intensity of the NIR transition, thus providing a simple 'tuning' mechanism for the optical properties of the complexes. Molecular orbital calculations using the ZINDO method have been carried out to support our assignments of the electronic transitions. The crystal structures of two of the new complexes, having 3-benzoylpyridine and 4-cyanopyridine ligands respectively, are also described.

Results and discussion

Syntheses and characterisation of complexes

The complexes **1**–**12** are shown in Scheme 1. This series of complexes was chosen with two aims in mind: firstly, what effect a variety of substituents (phenyl, chloro, acetyl, benzoyl, and cyano) would have on the general optical properties of the complexes, in particular the Mo → pyridine charge-transfer transitions; and secondly, what effect the position of this substituent on the pyridine ring would have on the detailed optical properties. Thus for each type of substituent two complexes were prepared, one with a 3-substituted pyridine and the other with a 4-substituted pyridine as ligand. Complex **1**, with a simple alkyl substituent, is our reference

compound for comparison with the others (it was not possible to use the complex with unsubstituted pyridine as our reference because it proved to be rather unstable, discolouring quickly and not giving very clean electrochemical results). Finally complex **12**, with an isoquinoline ligand, was also included as the more extended delocalised network of quinoline compared to pyridine should make it a better electron-acceptor.

All of the complexes were prepared by reaction of the appropriate pyridine derivative with either $[Mo(Tp^{Me,Me})(NO)Cl_2]$ in toluene (complex **1**) or $[Et_3NH][Mo(Tp^{Me,Me})(NO)Cl_2]$ (all other complexes) according to the published methods,[4] and purified by column chromatography on silica with various solvent systems (see Experimental section). For

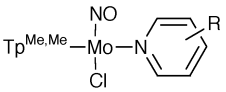

1 R = 4–CH(^{n}Bu)$_2$
2 R = 4–Ph
3 R = 3–Ph
4 R = 4–C(O)Ph
5 R = 3–C(O)Ph
6 R = 4–C(O)Me
7 R = 3–C(O)Me
8 R = 4–CN
9 R = 3–CN
10 R = 4–Cl
11 R = 3–Cl
12 RC_5H_4N = isoquinoline

Scheme 1

complex **1**, attachment of the pyridine ligand to the 16-electron $[Mo(Tp^{Me,Me})(NO)Cl_2]$ groups is accompanied by one-electron reduction of the Mo centre;[4a–c] in the other cases, the Mo starting material is reduced first to give $[Et_3NH][Mo(Tp^{Me,Me})(NO)Cl_2]$ to which the pyridine derivative can attach without the need for a simultaneous reduction.[4d] Either method works well. The complexes were characterised on the basis of their FAB mass spectra, elemental analyses and IR spectra; these data are all collected in Table 1. The FAB mass spectrum showed a peak corresponding to the molecular ion in every case, often with a fragment at $M^+ - 35$ corresponding to loss of the chloride ligand. IR spectra showed the usual ν_{NO} and ν_{BH} vibrations,[4,5] and also showed stretching vibrations characteristic of the carbonyl groups of **4**–**7** and the cyano groups of **8** and **9**.

Two of the complexes, **5** and **8**, have been structurally characterised (Fig. 1 and 2; Tables 2 and 3). They show the expected pseudo-octahedral geometries around the metal centre, with the bond lengths and angles in the metal coordination sphere showing very little difference between the two structures, and are generally similar to the other two structures of the [Mo(Tp*)(No)Cl(py)] series that have been reported.[4a,c] In the structure of **5** the 3-benzoylpyridine ligand is not planar but twisted such that the plane of the phenyl ring is 56° away from the plane of the pyridyl ring.

The electrochemical properties of the complexes are summarised in Table 4. All of the complexes undergo a chemically

Table 1 Characterisation data for the new complexes

			Elemental analyses (%)			IR spectral data/cm^{-1}			
	Colour	Yield (%)	C[a]	H	N	ν_{NO}	ν_{BH}	Others	FABMS (*m*/*z*)
1	Green	15	52.5(52.5)	6.5(6.8)	16.9(16.9)	1618	2543		665
2[b]	Brick red	55	49.0(49.0)	5.2(5.0)	17.1(17.3)	1611	2544		615
3	Green	52	50.7(50.9)	5.4(5.1)	18.2(18.3)	1614	2549		615
4	Purple	83	50.2(50.5)	4.8(4.9)	17.3(17.5)	1615	2544	1664[d]	643
5	Dark red	56	50.4(50.5)	5.0(4.9)	17.8(17.5)	1610	2544	1665[d]	643
6[c]	Purple	49	42.6(42.3)	4.5(4.8)	17.1(17.3)	1617	2547	1698[d]	581
7	Brown	33	45.4(45.6)	4.7(5.0)	19.6(19.3)	1625	2550	1690[d]	581
8	Blue	42	45.0(44.8)	4.7(4.7)	22.3(22.4)	1615	2545	2240[e]	564
9	Dark red	32	44.4(44.8)	4.3(4.7)	22.4(22.4)	1623	2547	2237[e]	564
10[b]	Brown	23	40.6(39.9)	4.2(4.4)	17.8(18.2)	1615	2547		573
11[b]	Brown	34	40.4(39.9)	4.4(4.4)	18.5(18.2)	1622	2553		573
12	Dark red	64	48.7(49.1)	5.3(5.0)	18.7(19.1)	1613	2547		589

[a] Calculated values in parentheses. [b] $0.5CH_2Cl_2$ used to balance elemental analysis. [c] $0.8CH_2Cl_2$ used to balance elemental analysis. [d] Carbonyl group. [e] Cyano group.

Table 2 Crystallographic data for the two crystal structures[a]

Compound	**5** · $1.5CH_2Cl_2$	**8** · $0.25C_6H_{14}$
Formula	$C_{28.5}H_{34}BCl_4MoN_8O_2$	$C_{22.5}H_{29.5}BClMoN_9O$
M	769.19	584.25
System, space group	Orthorhombic, *Fdd*2	Triclinic, $P\bar{1}$
a/Å	24.826(2)	8.3816(13)
b/Å	39.023(3)	12.774(3)
c/Å	14.233(4)	13.902(3)
α/°		108.66(2)
β/°		93.351(14)
γ/°		91.54(2)
U/Å^3	13 789(4)	1406.2(5)
Z	16	2
μ/mm^{-1}	0.730	0.593
Reflections collected: total, independent, R_{int}	21 987, 7756, 0.0592	12 252, 4933, 0.0168
Final R_1, wR_2 [b,c]	0.0511, 0.1185	0.0357, 0.1042

[a] Details in common: Mo-Kα radiation (0.710 73 Å); temperature for data collection, 173(2) K. [b] Structure was refined on F_o^2 using all data; the value of R_1 is given for comparison with older refinements based on F_o with a typical threshold of $F \geq 4\sigma(F)$. [c] $wR_2 = [\sum[w(F_o^2 - F_c^2)^2]/\sum w(F_o^2)^2]^{1/2}$ where $w^{-1} = [\sigma^2(F_o^2) + (aP)^2 + bP]$ and $P = [\max(F_o^2, 0) + 2F_c^2]/3$.

Table 3 Selected bond distances (Å) and angles (°) for the two new structures

$5 \cdot 1.5CH_2Cl_2$		$8 \cdot 0.25C_6H_{14}$	
Mo(1)–N(1)	1.906(6)	Mo(1)–N(51)	1.899(5)
Mo(1)–N(11)	2.175(5)	Mo(1)–N(12)	2.166(3)
Mo(1)–N(21)	2.179(4)	Mo(1)–N(22)	2.186(3)
Mo(1)–N(41)	2.185(4)	Mo(1)–N(41)	2.207(3)
Mo(1)–N(31)	2.263(4)	Mo(1)–N(32)	2.241(3)
Mo(1)–Cl(1)	2.412(2)	Mo(1)–Cl(1)	2.4200(12)
O(1)–N(1)	0.996(6)	O(52)–N(51)	0.977(4)
N(1)–Mo(1)–N(11)	94.7(2)	N(51)–Mo(1)–N(12)	96.64(11)
N(1)–Mo(1)–N(21)	97.1(2)	N(51)–Mo(1)–N(22)	96.26(11)
N(11)–Mo(1)–N(21)	85.5(2)	N(12)–Mo(1)–N(22)	83.07(10)
N(1)–Mo(1)–N(41)	91.1(2)	N(51)–Mo(1)–N(41)	89.48(11)
N(11)–Mo(1)–N(41)	92.1(2)	N(12)–Mo(1)–N(41)	171.42(9)
N(21)–Mo(1)–N(41)	171.7(2)	N(22)–Mo(1)–N(41)	90.31(10)
N(1)–Mo(1)–N(31)	177.1(2)	N(51)–Mo(1)–N(32)	175.78(11)
N(11)–Mo(1)–N(31)	83.4(2)	N(12)–Mo(1)–N(32)	87.46(10)
N(21)–Mo(1)–N(31)	84.97(14)	N(22)–Mo(1)–N(32)	83.22(10)
N(41)–Mo(1)–N(31)	86.83(14)	N(41)–Mo(1)–N(32)	86.34(9)
N(1)–Mo(1)–Cl(1)	92.02(13)	N(51)–Mo(1)–Cl(1)	92.32(9)
N(11)–Mo(1)–Cl(1)	173.30(12)	N(12)–Mo(1)–Cl(1)	93.83(7)
N(21)–Mo(1)–Cl(1)	93.12(13)	N(22)–Mo(1)–Cl(1)	171.16(7)
N(41)–Mo(1)–Cl(1)	88.34(11)	N(41)–Mo(1)–Cl(1)	91.92(7)
N(31)–Mo(1)–Cl(1)	89.90(11)	N(32)–Mo(1)–Cl(1)	88.39(7)

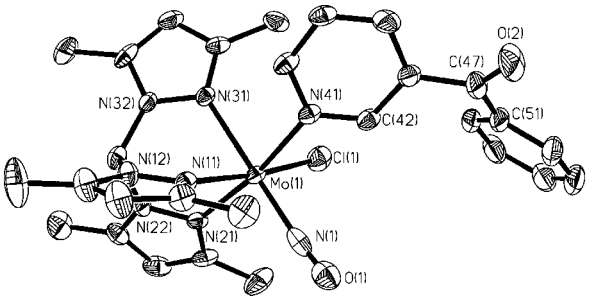

Fig. 1 Crystal structure of complex $5 \cdot 1.5CH_2Cl_2$.

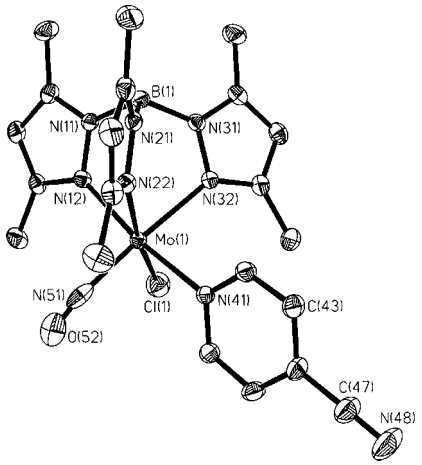

Fig. 2 Crystal structure of complex $8 \cdot 0.25C_6H_{14}$.

reversible reduction which is a one-electron reduction to the 18-electron mono-anion.[4] The redox potential of this process is clearly sensitive to the nature of the substituent on the pyridyl ligand. Addition of electron-withdrawing substituents at the pyridyl C^4 position makes the reduction easier, suggesting that the formally metal-centred reduction is in fact partly delocalised onto the π-accepting pyridyl group. Thus, changing an alkyl substituent (complex **1**) to a benzoyl substituent (complex **4**) results in a positive shift of the potential of the 17e/18e redox couple by 680 mV. Attaching the same substituent to the pyridyl C^3 position has a much weaker effect, *cf.* the difference of only 0.29 V between the redox potentials of complexes **1** and **5**. The difference between these two shifts (0.68 − 0.29 V = 0.39 V) represents the difference between the 3-substituted and the 4-substituted pyridines, and we term it here the 'substituent shift'. A similar effect, albeit of varying magnitude, can be seen for the other pairs of complexes: for the cyano-substituted complexes **8** and **9** the substituent shift is 0.23 V; for the acetyl-substituted complexes **6** and **7** it is 0.38 V, almost the same as for the benzoyl-substituted complexes; for the Cl-substituted complexes **10** and **11** it is 0.08 V; and finally for the phenyl-substituted complexes **2** and **3** the substituent shift is 0.08 V. It is clear from the electrochemical data that the most effective electron-withdrawing substitutents to stabilise the reduced forms of the complexes are the conjugated π-acceptor substituents benzoyl, acetyl and cyano (*cf.* complexes **4**, **6** and **8**). The electronegative Cl atom is in contrast much less effective at stabilising the reduced forms of these complexes and consequently the difference between its effect at the 3- and 4-positions of the pyridyl ligand is not so marked.

These 17e/18e redox couples gave symmetric waves in cyclic voltammograms, indicating chemical reversibility, which was subsequently confirmed by the spectroelectrochemical studies. The peak–peak separations of 100–200 mV in thf (at a scan

Table 4 Electrochemical properties of the new complexes[a]

Compound	Mo(I)/Mo(0)	Mo(I)/Mo(II)
1	− 2.20(150)	0.10(120)
2	− 2.00(140)	0.09(140)
3	− 2.08(150)	0.12(110)
4	− 1.52(150)	0.13(120)
5	− 1.91(140)	0.14(i)[b]
6	− 1.59(160)	0.14(140)
7	− 1.97(140)	0.12(i)[b]
8	− 1.55(190)	0.18(i)[b]
9	− 1.78(180)	0.17(i)[b]
10	− 2.03(180)	0.13(160)
11	− 1.95(130)	0.17(100)
12	− 2.05(200)	0.09(180)

[a] All measurements were made by cyclic voltammetry in thf containing 0.1 mol dm^{-3} $[^nBu_4N][BF_4]$ at a platinum bead working electrode. The scan rate was 0.1 V s^{-1}. All potentials are *vs.* the ferrocenium–ferrocene couple which was used as an internal reference. Values in parentheses are peak–peak separations in mV for the reversible processes (ΔE_p for the ferrocenium–ferrocene couple under the same conditions was about 140 mV). [b] Denotes an irreversible process.

rate of 0.1 V s^{-1}) are somewhat larger than the theoretical ideal of 59 mV, which is typical of these complexes[4] and may be ascribed to uncompensated solution resistance in a high-resistance solvent and/or slow electron-transfer kinetics. We note here that we have concentrated on the use of electron-withdrawing substituents in this study because such substituents make the reduction (and therefore the spectroelectrochemical studies) easier. Although it is perfectly possible to prepare complexes of this type with electron-donor substituents on the pyridine ring, the very negative potentials that result tend to be near the decomposition limit of the solvent/base electrolyte combination which prevents effective spectroelectrochemical studies.

The complexes also all undergo a one-electron oxidation to the 16-electron monocations (Table 4).[4] The potentials of these are much less sensitive to the presence of substituents on the pyridyl ligand, in keeping with our earlier suggestion that the oxidation occurs in an orbital which is much more localised on the metal ion than that involved in the reduction.[6] In most cases these 17e/16e couples are chemically reversible, but in a few cases the process is irreversible.

Spectroelectrochemical behaviour and ZINDO calculations on 1

To start with we will consider the behaviour of complex **1**, in which the pyridyl substituent is just an alkyl group. The lowest-energy electronic transitions at 472 and 415 nm (Table 5) we ascribe to two metal-to-ligand charge-transfer (MLCT) processes in which the acceptor orbital is the LUMO of the π-acceptor pyridine ligand. The presence of two such transitions is consistent with the splitting of the d(π) orbital set by interaction with the strongly π-accepting nitrosyl ligand, such that d_{xz} and d_{yz}, which are approximately degenerate, are filled and lie below the singly-occupied d_{xy} orbitals. The transitions at 472 nm and 415 nm can therefore be assigned as $d_{xy} \rightarrow$ py and (d_{xz}, d_{yz}) → py transitions. Also present is a ligand-centred $\pi \rightarrow \pi^*$ transition in the UV region at 277 nm, which has a low-energy shoulder at *ca.* 320 nm whose nature is uncertain.

On oxidation of **1** to the 16-electron cation $[\mathbf{1}]^+$ in an OTTLE cell,[7] resulting formally in formation of a low-spin d^4 Mo(II) complex, two new transitions appear: a weak one at 776 nm and a very strong one at 407 nm (Fig. 3). The former is a d–d transition from the filled d_{xz}/d_{yz} levels to the now empty d_{xy} orbital. The expression 'd–d' is of course approximate because the d_{xz}/d_{yz} orbitals (taking the Mo–NO vector as the *z*-axis)[4c] have been lowered in energy by interaction with the two nitrosyl π* orbitals such that they are of mixed character, whereas d_{xy} cannot interact with a nitrosyl π* orbital in this way and has more pure d-orbital character (Fig. 4). A ZINDO molecular orbital calculation[8] was performed using a CAChe workstation on the model complex $[Mo(Tp^{Me,Me})(NO)Cl(C_5H_5N)]^+$ containing (for calculational simplicity) an unsubstituted pyridine ligand, and the results were used to calculate the electronic spectrum of the complex. The model complex was built with the Editor and was then energy-minimised using the molecular mechanics method with standard MM2 parameters; the calculated bond distances and angles in the energy-minimised structure are very similar to those of crystallographically characterised complexes such as **5** and **8**.

The ZINDO calculation predicts the weak 'd–d' transition at *ca.* 1000 nm (observed for $[\mathbf{1}]^+$: 776 nm), and a much stronger transition at 340 nm (observed for $[\mathbf{1}]^+$: 407 nm) which is a manifold containing overlapping ligand-to-metal charge-transfer transitions from the tris(pyrazolyl)borate and chloride ligands to the empty d_{xy} orbital on the oxidised metal centre. The agreement with the absolute energies we observed is only moderate, which is not surprising considering the semi-

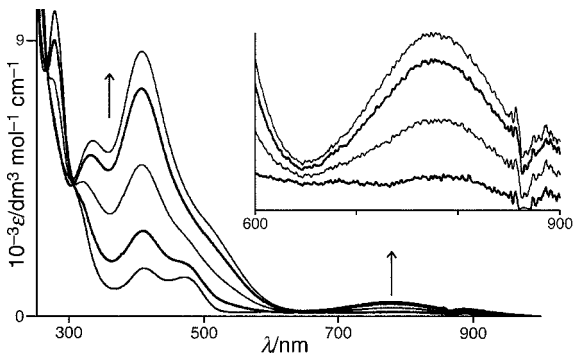

Fig. 3 Electronic spectra recorded during oxidation of **1** to $[\mathbf{1}]^+$.

Table 5 Electronic spectra in thf of complexes in their neutral [Mo(I), 17-electron] and reduced [Mo(0), 18-electron] oxidation states

Complex	λ_{max}/nm (10^{-3} ε/dm^3 mol^{-1} cm^{-1})					
1		277(10)	320 (sh)	415(1.5)[a]	472(1.3)[a]	
2		274(25)	341(4.0)	443(0.9)[a]	520(1.8)[a]	
3	248(25)	277 (sh)	337 (sh)	428(1.0)[a]	490(1.3)[a]	
4		260(19)	361(2.4)	574(1.8)[a]	660 (sh)[a]	
5		260(25)	350 (sh)	405(1.0)[a]	511(1.0)[a]	
6		280(8.5)	362(2.4)	574(2.1)[a]	670 (sh)[a]	
7	260 (sh)	280 (sh)	340 (sh)	405 (sh)[a]	512(1.2)[a]	
8	242(15)	279 (sh)	369(2.7)	584(2.6)[a]	670 (sh)[a]	
9	260(12)	280(11)	340(2.4)	430 (sh)[a]	532(1.5)[a]	
10		280(8.0)	324 (sh)	429(1.1)[a]	499(1.3)[a]	
11		279(7.9)	332 (sh)	432(1.0)[a]	505(1.3)[a]	
12		280(11)	315(5.2)		533(1.5)[a]	
$[\mathbf{1}]^-$	264 (sh)	327(6.7)	394(4.1)	550 (sh)	830(12.0)[b]	
$[\mathbf{2}]^-$	265(10.4)	340 (sh)	370(8.9)	448(5.7)	832(16.9)[b]	
$[\mathbf{3}]^-$	260(16.7)	321(4.0)		410(3.9)	758(9.6)[b]	
$[\mathbf{4}]^-$	255(10.8)	325(3.5)	428(4.8)	517(8.4)	695(12.9)[b]	
$[\mathbf{5}]^-$			361 (sh)	477(2.3)	717(5.3)[b]	1514(2.5)[b]
$[\mathbf{6}]^-$	250 (sh)	358(5.2)	450(5.9)	502(5.9)	657(11.6)[b]	
$[\mathbf{7}]^-$	258 (sh)	340 (sh)		433(3.6)	722(8.9)[b]	1274(2.4)[b]
$[\mathbf{8}]^-$	260 (sh)	328(6.2)	376(4.0)	433(6.9)	633(10.2)[b]	
$[\mathbf{9}]^-$			314(3.7)	433(2.8)	688(5.4)[b]	≈1050 (sh)[b]
$[\mathbf{10}]^-$	260 (sh)		320(3.7)	412(3.7)	774(8.9)[b]	
$[\mathbf{11}]^-$			322(3.3)	412(3.4)	725(7.2)[b]	
$[\mathbf{12}]^-$	260 (sh)		356 (sh)	445(3.5)	719(9.0)[b]	920 (sh)[b]

[a] MLCT transitions in the 17-electron complexes. [b] MLCT transitions in the reduced 18-electron complexes.

empirical nature of the ZINDO method, but most importantly the natures of the two new transitions can be assigned confidently.

On reduction of **1** to the 18-electron anion $[\mathbf{1}]^-$ in the OTTLE cell, resulting formally in formation of a low-spin d^6 Mo(0) complex, a dramatic change takes place in the spectrum: a strong new transition appears at 830 nm (ε *ca.* 12 000 $dm^3\ mol^{-1}\ cm^{-1}$) (Fig. 5, Table 5). We ascribe this to a Mo → pyridine MLCT transition, enhanced in intensity compared to neutral **1** because the more electron-rich nature of the metal centre results in an increased transition dipole moment for the MLCT transition, and lowered in energy because of the raising of the metal-centred d(π) orbitals on reduction nearer to the ligand-centred LUMO. Confirmation of this assignment is again provided by a ZINDO molecular orbital calculation on $[Mo(Tp^{Me,Me})(NO)Cl(C_5H_5N)]^-$ which clearly shows the HOMO to be a metal-centred d-orbital (d_{xy}, taking the Mo–NO vector as the *z*-axis) and the LUMO to be an antibonding orbital of the pyridine ligand. The ZINDO calculation predicts that this MLCT transition should be at 630 nm (observed for $[\mathbf{1}]^-$, 830 nm). The absolute agreement of the transition energy is not good but again the character of the HOMO and LUMO, and the fact that this new transition is an MLCT transition to the pyridyl ligand, are quite clear.

It was apparent from this work that the redox activity of complexes of type **1**, and the presence of a strong, low-energy absorption in the reduced form of the complex, provided a good basis for a new class of electrochemically switchable (electrochromic) near-IR dyes.[2] This stimulated our interest in the spectroelectrochemical properties of the other members of this series, which are discussed in the next section.

Spectroelectrochemical behaviour and ZINDO calculations on the other complexes

The electronic spectra of the other neutral 17-electron complexes follow the same general pattern as that of **1**, with intense ligand-centred transitions in the UV region (<300 nm), a poorly resolved transition of uncertain origin between 310 and 370 nm, and (usually) two Mo → pyridyl MLCT transitions at the lower-energy end of the spectrum in the visible region. These MLCT transitions are sensitive to the nature and position of the substituents on the pyridyl ligand. Thus, addition of the 4-benzoyl substituent to the pyridine ligand in **4** results in the MLCT transition being red-shifted from 472 nm to 574 nm as the pyridyl-based LUMO is lowered in energy. In contrast attaching the same substituent to the pyridyl C^3 position in **5** has a predictably weaker effect (*cf.* the electrochemical measurements), moving the MLCT transition to 511 nm. This pattern is preserved in the other complexes, with the various electron-withdrawing substituents moving the lowest-energy MLCT maximum to the 500–580 nm range, compared to 472 nm for complex **1**.

On reduction of these complexes to the 18-electron monoanions, in every case a strong new MLCT transition appears at the low-energy end of the spectrum (Table 5, Fig. 5–7). The positions of these transitions show some interesting patterns.

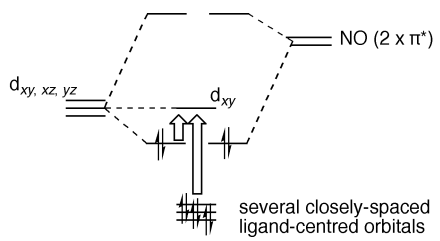

Fig. 4 Frontier orbitals of $[Mo(Tp^{Me,Me})(NO)Cl(C_5H_5N)]^+$. The d–d transition and the LMCT transition which appear in the oxidised form of the complexes are indicated as transparent vertical arrows.

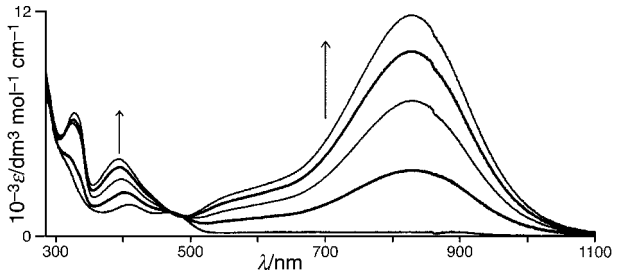

Fig. 5 Electronic spectra recorded during reduction of **1** to $[\mathbf{1}]^-$.

Firstly, attachment of an electron-withdrawing substituent at the pyridyl C^4 position *increases* the energy of the principal MLCT transition; for example comparison of **1** and **8** shows that replacement of an alkyl group by a cyano group in the same position results in the MLCT transition in the reduced species moving from 830 nm to 633 nm, and a similar effect occurs with the carbonyl substituents of **4** and **6** (λ_{max} = 695 and 657 nm respectively); the spectrum of $[\mathbf{4}]^-$ is in Fig. 6. This is exactly contrary to the behaviour shown by the neutral 17-electron complexes, where an electron-withdrawing substituent at the C^4 position of the pyridyl ring caused a red-shift of the lowest-energy MLCT as explained above. We ascribe this to improved mixing between the metal d(π) and pyridyl π^* orbitals, because in the reduced state the metal orbitals will be raised in energy compared to the neutral 17-electron precursors, and can therefore interact more strongly with the pyridine π^* orbitals resulting in greater separation after mixing. A similar effect is seen in comparison of $[Ru(bipy)_2(sq)]^+$ and $[Ru(bipy)_2(q)]^{2+}$ (sq = 1,2-benzosemiquinone anion, q = 1,2-benzoquinone); although q is a better electron acceptor than sq, the Ru → q MLCT energy is considerably higher than the Ru → sq MLCT energy because greater mixing between metal and ligand orbitals results in a larger HOMO–LUMO gap.[9]

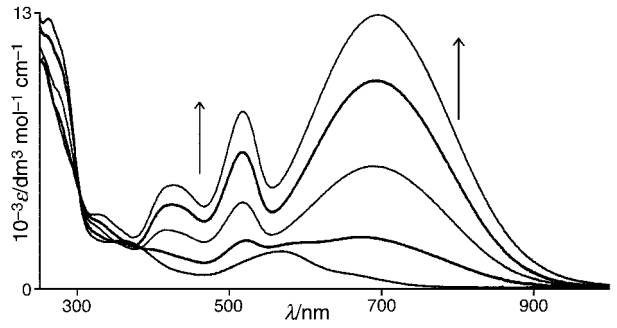

Fig. 6 Electronic spectra recorded during reduction of **4** to $[\mathbf{4}]^-$.

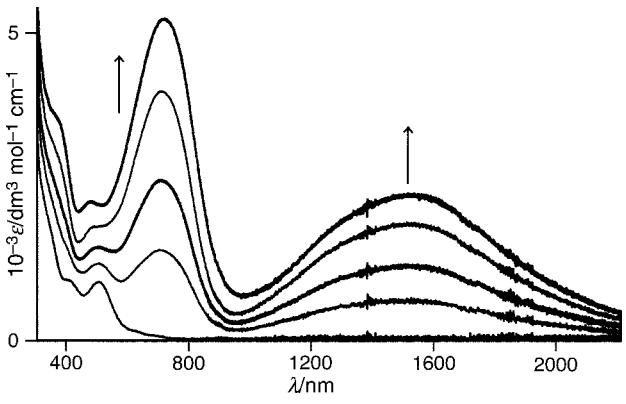

Fig. 7 Electronic spectra recorded during reduction of **5** to $[\mathbf{5}]^-$.

The second point to notice is that when there is a conjugated electron-withdrawing substituent at the 3-position rather than the 4-position of the pyridyl ring (a benzoyl group in **5**, an acetyl group in **7** and a cyano group in **9**) there is an additional weaker MLCT transition at lower energy (1514, 1274 and ≈1100 nm respectively), in the near-IR region of the spectrum. Fig. 7 shows the electronic spectra recorded during reduction of **5** to $[\mathbf{5}]^-$, which may be compared with Fig. 6 which depicts the spectrum of the isomeric complex $[\mathbf{4}]^-$. We had expected that changing the pyridyl substituent from C^4 to C^3 would affect the energy of the Mo → pyridyl MLCT transition (which it does; see Table 5), but had not expected that an *additional* transition would result. The origin of this effect is clear from the ZINDO results, which show that in the complexes having 3-substituted pyridine ligands, the lower symmetry of the ligand results in the lowest two π* orbitals (LUMO and LUMO + 1) being close together, such that two low-energy Mo → pyridyl MLCT transitions can occur. In contrast in the complexes with the 4-substituted pyridyl ligands, there is a much larger gap between the first and second π* orbitals of the pyridyl ring which means that there is only one low-energy Mo → pyridyl MLCT transition, with the next highest presumably in a region of the spectrum which is already crowded with other transitions. Fig. 8 shows the predicted electronic spectra based on the ZINDO computation for complexes $[\mathbf{6}]^-$ and $[\mathbf{7}]^-$, together with the real spectra. The predicted energies for the MLCT transitions are consistently too high but qualitatively the agreement is reasonable, and in particular the additional low-energy transition (labelled * in the figure) appears in the calculated spectrum of $[\mathbf{7}]^-$ but not in the calculated spectrum of $[\mathbf{6}]^-$.

A simple illustration of the origin of this effect is in Fig. 9, which shows the lowest two antibonding orbitals for 3-acetylpyridine and 4-acetylpyridine based on an extended-Hückel calculation. For 3-acetylpyridine the two orbitals are quite close together in energy because each of them encompasses one electronegative atom (O or N); for 4-acetylpyridine the LUMO encompasses both the acetyl O atom and the pyridyl N atom, and is therefore much lower in energy than LUMO + 1 which is based on carbon atoms only. From this it is easy to understand the presence of a second low-energy

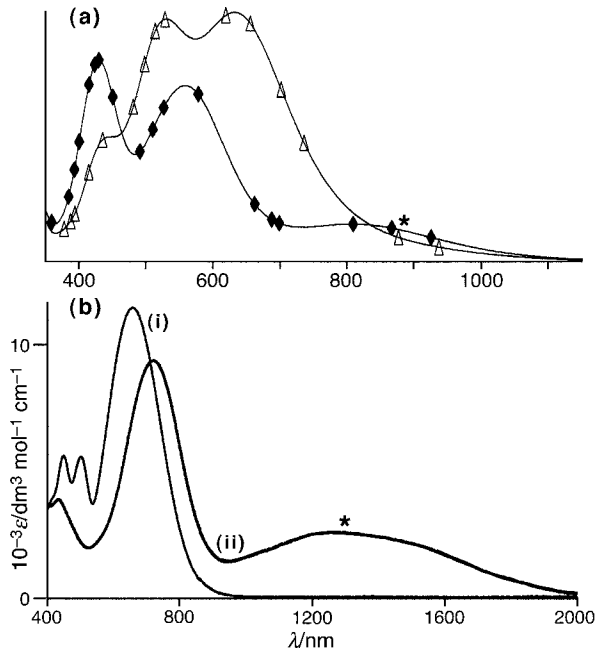

Fig. 8 (a) Calculated (based on ZINDO analyses), and (b) actual electronic spectra of (i) $[\mathbf{6}]^-$ and (ii) $[\mathbf{7}]^-$. For the calculated spectra, the hollow triangles denote the spectrum of $[\mathbf{6}]^-$ and the black diamonds denote the spectrum of $[\mathbf{7}]^-$.

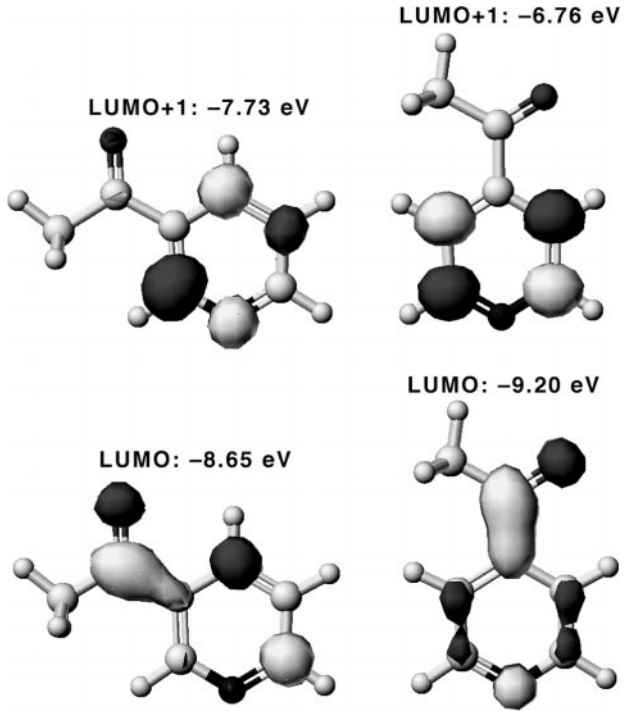

Fig. 9 The lowest two antibonding orbitals of 3-acetylpyridine and 4-acetylpyridine, calculated by the extended-Hückel method.

Mo → pyridyl MLCT transition for **5**, **7** and **9** but not for **4**, **6** and **8**.

With regard to the complexes containing other substituents, comparison of **2** and **3** (4-phenyl and 3-phenyl substituents) shows the importance of the substituent being a strong π-acceptor group. Complex $[\mathbf{3}]^-$ shows no obvious additional MLCT transition compared to $[\mathbf{2}]^-$, although the tail of the principal MLCT transition of $[\mathbf{3}]^-$ at 758 nm does extend much further into the near-IR region than does the analogous transition of $[\mathbf{2}]^-$, indicating that there is indeed an additional lower-energy transition but that it is weak and not properly resolved. Complex $[\mathbf{12}]^-$ also shows two clear MLCT transitions, at 719 and 920 nm, suggesting again (as for the 3-substituted pyridyl ligands of $[\mathbf{5}]^-$, $[\mathbf{7}]^-$ and $[\mathbf{9}]^-$) that the low symmetry of the isoquinoline ligand results in two closely-spaced π* orbitals. Finally, comparison of the spectra of $[\mathbf{10}]^-$ and $[\mathbf{11}]^-$ shows that moving the Cl substituent from the 4-position to the 3-position of the pyridyl ligand does not result in any sign of an additional low-energy MLCT transition, which is to be expected as it does not have the necessary π-acceptor character.

Conclusions

In summary we have investigated the spectroelectrochemical behaviour of an extensive series of complexes of the type $[Mo(Tp^{Me,Me})(NO)Cl(py)]$, and have made two significant findings. Firstly in the reduced forms of these complexes there is always an intense, low-energy MLCT transition from the reduced metal centre to the LUMO of the pyridyl ligand. These transitions have extinction coefficients of up to *ca.* 10 000 dm^3 mol^{-1} cm^{-1} and occur at the red end of the visible spectrum. Compared to other electrochromic near-IR dyes[1–3] this effect is not spectacular. However, our second principal finding is that attachment of a conjugated, electron-withdrawing substituent (especially a carbonyl group) at C^3 of the pyridyl ligand rather than the C^4 position results in the presence of a second MLCT transition which is well into the NIR region of the spectrum; for example complexes $[\mathbf{5}]^-$ (with a 3-benzoylpyridine ligand) has an absorption maximum at 1514 nm. This is of considerable significance for the devel-

opment of materials for electro-optic switching, and we are currently pursuing this.

Acknowledgements

We thank the European Community TMR Network programme (contract no. EC-CHRX-CT96-0047) and the EPSRC (UK) for financial support.

Experimental

General details

All of the substituted pyridines and isoquinoline used as ligands were purchased from the usual commercial sources (Aldrich, Avocado, Lancaster) and used as received. Instrumentation used for standard spectroscopic measurements, cyclic voltammetry and spectroelectrochemical measurements has been described previously.[7] All electrochemical measurements were made using thf as solvent at room temperature. Spectroelectrochemical studies were carried out in thf at −30 °C, and the chemical reversibility of all processes was confirmed by reversing the applied potential and regenerating the spectrum of the starting material.

Syntheses

Complex 1. This was prepared by reaction of $[Mo(Tp^{Me,Me})(NO)Cl_2]$ (0.50 g, 1.01 mmol), 4-(1-butylpentyl) pyridine (2 cm^3, excess) and dry Et_3N (1 cm^3) in toluene (40 cm^3) at 85 °C under N_2 for 2 h. After cooling the reaction mixture and removal of the solvent *in vacuo*, the crude material was purified by chromatography on silica gel using CH_2Cl_2–hexane (9 : 1) as eluent; the major green band was collected and finally recrystallised from CH_2Cl_2–hexane.

Complexes 2–12. These were prepared by reaction of $[Et_3NH][Mo(Tp^{Me,Me})(NO)Cl_2]$ with the appropriate pyridine ligand (2 equivalents) in toluene at reflux inder N_2 for 24 h. The reaction was then worked up and purified by chromatography as above, eluting with pure CH_2Cl_2 (for **9**) or CH_2Cl_2 containing 0.5% thf (all other complexes). The major coloured band was collected (see Table 1 for colours of complexes), the solvent removed *in vacuo*, and the complex finally recrystallised from CH_2Cl_2–hexane. For complexes **5** and **8**, X-ray quality crystals were obtained.

All routine characterisation data for the new complexes are collected in Table 1.

Crystallography

Suitable crystals were quickly transferred from the mother-liquor to a stream of cold N_2 on a Siemens SMART diffractometer fitted with a CCD-type area detector. In all cases a full sphere of data was collected at −100 °C using graphite-monochromatised Mo-Kα radiation. A detailed experimental description of the methods used for data collection and integration using the SMART system has been published.[10] Empirical absorption corrections were applied using SADABS,[11] and structure solution and refinement was performed with the SHELX suite of programs.[12] Table 2 contains a summary of the crystal parameters, data collection and refinement.

For both structures, the metal complex core refined with no problems; the only difficulties in each case arose from lattice solvent molecules. For $\mathbf{5}\cdot 1.5CH_2Cl_2$, one CH_2Cl_2 is disordered over two sites such that the carbon atom C(1) has 100% site occupancy, with the two Cl atoms each being split between two sites with 50% site occupancy. The second molecule of CH_2Cl_2 is not disordered but refined with 50% site occupancy for all atoms. Restraints were applied to the C–Cl distances, and also to the thermal parameters of all atoms in these CH_2Cl_2 molecules, to keep the refinement stable. For $\mathbf{8}\cdot 0.25C_6H_{14}$ the asymmetric unit contains three carbon atoms adjacent to an inversion centre which appeared to constitute half of a hexane molecule, but these refined with site occupancies of only 50% each, resulting in 0.25 hexane molecules *per* complex.

CCDC reference number 440/130. See http://www.rsc.org/suppdata/nj/1999/915/ for crystallographic data in .cif format.

References

1 (*a*) A. M. Barthram, R. L. Cleary, R. Kowallick and M. D. Ward, *Chem. Commun.*, 1998, 2695; (*b*) S.-M. Lee, M. Marcaccio, J. A. McCleverty and M. D. Ward, *Chem. Mater.*, 1998, **10**, 3272; (*c*) N. C. Harden, E. R. Humphrey, J. C. Jeffery, S.-M. Lee, M. Marcaccio, J. A. McCleverty, L. H. Rees and M. D. Ward, *J. Chem. Soc., Dalton Trans.*, 1999, 2417.
2 R. J. Mortimer, *Chem. Soc. Rev.*, 1997, **26**, 147; R. J. Mortimer, *Electrochim. Acta*, 1999, **44**, 2971.
3 (*a*) M. Emmelius, G. Pawlowski and H. W. Vollmann, *Angew. Chem., Int. Ed. Engl.*, 1989, **28**, 1445; (*b*) J. Fabian and R. Zahradnik, *Angew. Chem., Int. Ed. Engl.*, 1989, **28**, 677; (*c*) J. Fabian, H. Nakazumi and M. Matsuoka, *Chem. Rev.*, 1992, **92**, 1197.
4 (*a*) A. Das, J. C. Jeffery, J. P. Maher, J. A. McCleverty, E. Schatz, M. D. Ward and G. Wollermann, *Inorg. Chem.*, 1993, **32**, 2145; (*b*) A. Das, J. P. Maher, J. A. McCleverty, J. A. Navas Badiola and M. D. Ward, *J. Chem. Soc., Dalton Trans.*, 1993, 681; (*c*) S. L. W. McWhinnie, J. A. Thomas, T. A. Hamor, C. J. Jones, J. A. McCleverty, D. Collison, F. Mabbs, C. J. Harding, L. Yellowlees and M. G. Hutchings, *Inorg. Chem.*, 1996, **35**, 760; (*d*) S. L. W. McWhinnie, C. J. Jones, J. A. McCleverty, D. Collison and F. E. Mabbs, *Polyhedron*, 1992, **11**, 2639.
5 (*a*) A. M. W. Cargill Thompson, D. Gatteschi, J. A. McCleverty, J. A. Navas, E. Rentschler and M. D. Ward, *Inorg. Chem.*, 1996, **35**, 2701; (*b*) V. A. Ung, A. M. W. Cargill Thompson, D. A. Bardwell, D. Gatteschi, J. C. Jeffery, J. A. McCleverty, F. Totti and M. D. Ward, *Inorg. Chem.*, 1997, **36**, 3447.
6 J. A. McCleverty and M. D. Ward, *Acc. Chem. Res.*, 1998, **31**, 842.
7 S.-M. Lee, R. Kowallick, M. Marcaccio, J. A. McCleverty and M. D. Ward, *J. Chem. Soc., Dalton Trans.*, 1998, 3443.
8 ZINDO version 4.0.2 in the CAChe system; Oxford Molecular, Oxford, 1998.
9 M. Haga, E. S. Dodsworth and A. B. P. Lever, *Inorg. Chem.*, 1986, **25**, 447.
10 P. L. Jones, A. J. Amoroso, J. C. Jeffery, J. A. McCleverty, E. Psillakis, L. H. Rees and M. D. Ward, *Inorg. Chem.*, 1997, **36**, 10.
11 G. M. Sheldrick, SADABS, A program for absorption correction with the Siemens SMART area-detector system, University of Göttingen, 1996.
12 SHELXTL 5.03 program system, Siemens Analytical X-Ray Instruments, Madison, WI, 1995.

Paper 9/04599F